Bioactive Materials 4 (2019) 8–16

Contents lists available at ScienceDirect

Bioactive Materials

journal homepage: http://www.keaipublishing.com/biomat

# Effects of deformation twinning on the mechanical properties of biodegradable Zn-Mg alloys

Shiyang Liu[a,d], Damon Kent[a,b,c,d], Nghiem Doan[b,e], Matthew Dargusch[a,b,d], Gui Wang[a,b,d,*]

[a] School of Mechanical and Mining Engineering, The University of Queensland, St Lucia, 4072, Australia
[b] Centre for Advanced Materials Processing and Manufacturing (AMPAM), The University of Queensland, St Lucia, 4072, Australia
[c] School of Science and Engineering, University of the Sunshine Coast, Maroochydore, DC, 4558, Australia
[d] ARC Research Hub for Advanced Manufacturing of Medical Devices, The University of Queensland, St Lucia, 4072, Australia
[e] School of Dentistry and Oral Health, Griffith University, Gold Coast, 4215, Australia

ARTICLE INFO

*Keywords:*
Biodegradable metals
Zn-Mg alloys
Deformation twinning
Mechanical properties
Hot rolling

ABSTRACT

To satisfy the property requirements for biodegradable medical implants, Zn alloyed with low levels of Mg (≤0.8 wt%) has attracted increased research interest. In the present study, deformation twinning was observed in tensile tests and twinning appears to have an adverse impact on ductility. The profuse twinning in the as-cast Zn-Mg alloys accelerated crack growth in tension due to twinning impingement which caused local stress concentrations and initiates cracking. As-rolled Zn-Mg alloys have better ductility than their as-cast counterparts due to the inhibition of twinning by the refined $Mg_2Zn_{11}$ intermetallic phase and the finer grain size.

## 1. Introduction

Metallic medical implants are implanted into the body in order to improve human life by maintaining the function and/or healing damaged tissue [1]. Currently, most are permanent implants made from metallic materials including stainless steels, Co-based alloys and Ti-based alloys [2–5]. However, after healing the presence of the foreign implant materials in the body can cause chronic deleterious and inflammatory responses, and secondary surgery to remove such materials imparts additional risks to the patient and imposes significant further cost [4]. To overcome the deficiencies of permanent implants, biodegradable implants, intended to degrade in vivo gradually, have received considerable research attention. These biodegradable implants must have good biocompatibility (i.e. do not activate inflammatory responses and must be non-toxic) and the implant must fulfil its function for the full duration of the recovery phase [3,6–8]. Biodegradable metals (BMs) offer an innovative means to develop implants that are not permanent for orthopaedic applications, cardiovascular stents and other medical devices which have attracted increasing attention in recent decades [3,4,6,8–11].

Alloyed Fe and Mg, have been extensively investigated as good candidates for BMs because of their good biocompatibility [3,8,9,11]. However, their suitability for use in biodegradable medical implants is limited in some cases due to their degradation behaviour and its impact on the surrounding tissues. Iron-based metals exhibit low degradability, often slower than required to treat the patient and complications including mild inflammation and thrombogenicity have been reported as a consequence of their breakdown in previous studies [3,4]. In turn, rapid degradability impacts on the suitability of Mg-based BMs and the large amounts of hydrogen gas released as a result of their corrosion can adversely impact on healing, restricting the use of Mg based alloys in biodegradable medical implants [9,10,12–14]. Recently, Zn based alloys have emerged as a new candidate for BMs because of (1) its moderate degradability (i.e. 0.011–0.018 mm $year^{-1}$ in Hank's solution) [4,13,15]; (2) low melting point and low chemical reactivity which make Zn-based materials easy to cast and alloy [11]; (3) it is an essential trace element in the body which is critical to cell growth and facilitates wound healing [4,15–18]. However, a significant limitation for the application of Zn-based BMs is their inadequate mechanical properties. The tensile strength of as-cast pure Zn is 30 MPa, and the plasticity is below 2% [4,5]. This is well below the mechanical performance typically required for medical implants (ultimate tensile strength (UTS) ~ 200–300 MPa and elongation (ε) ~ 15%) [7].

To improve the suitability of Zn-based BMs for medical implants in respect to their mechanical performance, various approaches including alloying, different forming techniques and surface modification have been investigated [2,15,19]. Amongst these, Zn alloyed with Mg has been identified as a potential material for BMs. Yao et al. [14] reported

Peer review under responsibility of KeAi Communications Co., Ltd.
* Corresponding author. School of Mechanical and Mining Engineering, The University of Queensland, St Lucia, 4072, Australia.
*E-mail address:* gui.wang@uq.edu.au (G. Wang).

https://doi.org/10.1016/j.bioactmat.2018.11.001
Received 22 October 2018; Received in revised form 14 November 2018; Accepted 14 November 2018
Available online 23 November 2018

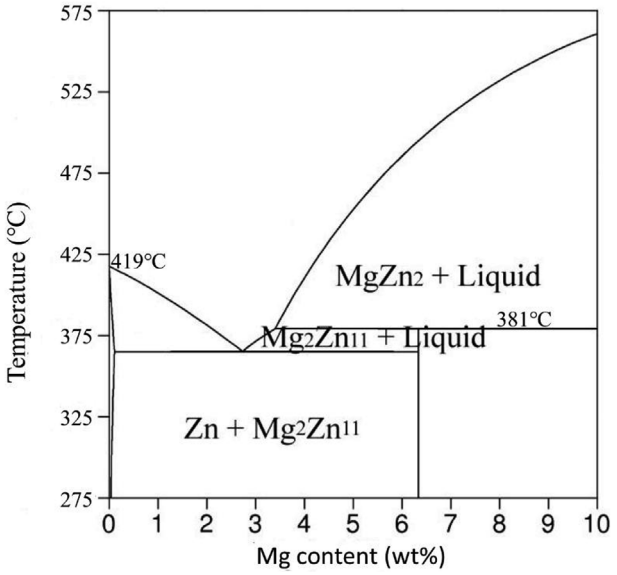


**Fig. 1.** Zn-Mg phase diagram [25].

that Zn alloyed with Mg contents below 10% offers significantly improved corrosion properties, i.e. the rate of corrosion is significantly lower compared with pure Zn, which allows the implanted Zn-Mg alloy to maintain its mechanical integrity for an appropriate time to fix the damaged tissue. The improvement in corrosion resistance was primarily attributed to the influence of the intermetallic phases ($Mg_2Zn_{11}$ and $MgZn_2$) which promote formation of an electrochemically inert protective film, such as $Mg_2(OH)_2CO_3$, on the surface of the Zn-Mg alloys [15]. In particular, as-cast Zn-3wt%Mg alloys were reported to offer a well-refined nanostructure and good corrosion resistance [4,20]. Furthermore, other studies report that the Zn alloyed with 1 wt% Mg provides the best combination of strength and ductility (UTS ~ 250 MPa and ε ~ 12%) for this alloy system [4]. The previous research suggested that a more substantial content of Mg (≤3 wt%) increase the volume fractions of the eutectic phase, improving the strength and hardness but undermining ductility [12,15]. The eutectic concentration for Mg in Zn is around 3 wt% while the maximum solubility of Mg in Zn is 0.1% (Fig. 1). The intermetallic compound formed in hypoeutectic Zn-Mg (≤3 wt%) alloys is $Mg_2Zn_{11}$, a hard and brittle eutectic phase, which is distributed within the softer α-Zn matrix. The low levels of ductility exhibited for the Zn-Mg alloys is considered insufficient for medical implant applications and this in conjunction with non-uniform breakdown due to preferential corrosion of the Mg has so far restricted the use of these alloys for BMs [6,8]. Hence, research interest has increasingly turned to Zn alloys with low contents of Mg (≤1 wt% Mg) to reduce the proportions of intermetallic phase in conjunction with appropriately designed processing to improve the mechanical and corrosion properties [21,22,23]. Gong et al. [12] reported that hot extrusion can improve the uniformity of biodegradation and mechanical properties (UTS ~ 250 MPa and ε ~ 12%) of Zn-1wt%Mg and the alloy's good biocompatibility was confirmed by in vitro cytotoxicity tests. Moreover, there are various studies reporting on the mechanical properties, corrosion properties, cytotoxicity of the Zn-1wt%Mg alone and with other elements such as Mn, Ca, and Sr fabricated by a range of different techniques [4,12,15,17,18,20,24]. Recently, Kubásek [17] reported that as-extruded Zn-0.8 wt%Mg has a suitable balance of strength (UTS ~ 301 MPa) and ductility (ε ~ 15%) while Mostaed et al. [15] reported good mechanical properties in as-extruded Zn-0.5 wt%Mg (UTS ~ 297 MPa and ε ~ 13%) and Zn-0.15 wt%Mg (UTS ~ 250 MPa and ε ~ 22%) alloys. The enhanced ductility is primarily attributed to the relatively low levels of Mg and associated reductions in the proportion of the brittle eutectic phase present in comparison to previously studied alloys [15,17].

Also, the inadequate mechanical properties of Zn and its alloys due to their low formability in the deformation processing, which is attributed to their hexagonal close-packed (HCP) crystal structure and lack of sufficient slip modes in plastic deformation [26]. The natural slip modes in HCP metals are slip on basal and prismatic planes, which are not sufficient to satisfy Von Mises criterion [27]. In some HCP metals, deformation may be accommodated through pyramidal slip dislocations, but pyramidal slip dislocations in Zn demand high critical resolved shear stress values due to the high c/a ratio of Zn [26,27]. Therefore, deformation twinning, another fundamental plastic deformation mode, plays an essential role in sustaining plastic strain in the deformation processing of Zn. In order to research the role of deformation twinning on mechanical properties of Zn-Mg alloys, studies on the nature of twinning in Zn-Mg alloys are essential. It is well known that $\{10\bar{1}2\} < 10\bar{1}\bar{1} >$ twinning is the only active twinning system in pure Zn due to its limited ductility and it is a contraction twinning mode because of the high c/a ratio of Zn (Fig. 2) [24,26–28]. There is little research on the twinning modes of Zn-Mg alloys currently, however, the twinning modes for dilute Zn-Mg alloys can be related to the deformation mechanisms for pure Zn. Previous research has

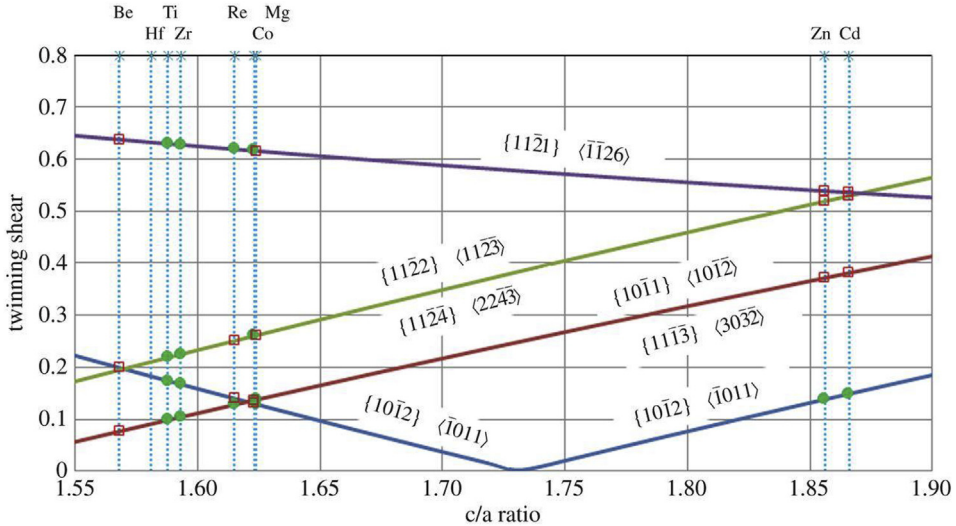


**Fig. 2.** Variation of twinning shear with the c/a ratio. Filled green circles indicate that this is an active twinning modes and red squares represent inactive twinning modes for the materials [28].

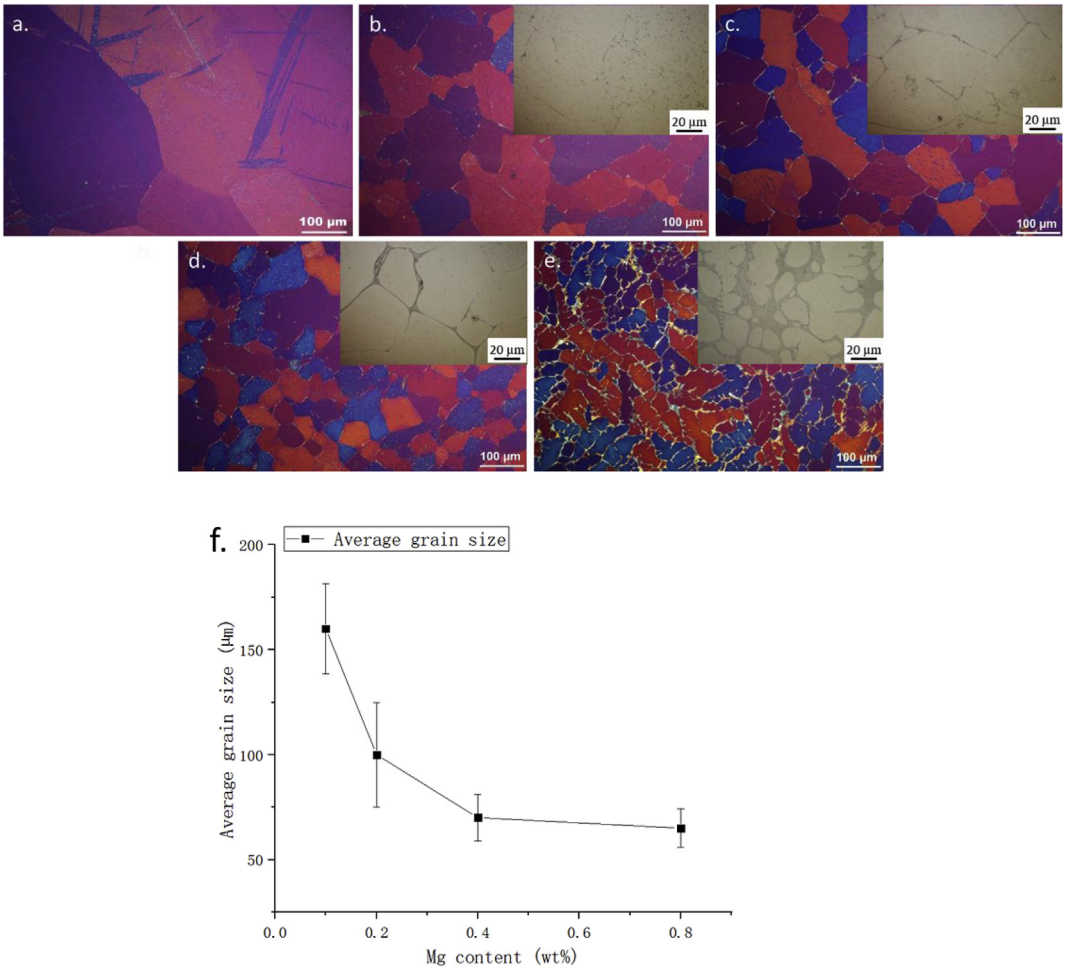


**Fig. 3.** The microstructure of the as-cast Zn and Zn-Mg alloys: (a) pure Zn, (b) Zn-0.1 wt%Mg, (c) Zn-0.2 wt%Mg, (d) Zn-0.4 wt%Mg (e) Zn-0.8 wt%Mg, and (f) the average grain size of Zn-Mg alloys. (The polarized micrographs are used to highlight grain structure and insets show the eutectic phase.)

demonstrated that deformation twinning improves the microstructure and consequently enhances mechanical properties of pure Zn by refining coarse grain structures during low strain rate deformation processing by subdivision of the grains and facilitating grain reorientation [29,30]. Since smaller grains inhibit twinning, deformation twinning ceases below a critical grain size [31]. The present study investigates the factors that affect the propensity and formation of twinning in pure Zn and Zn-Mg alloys in tension and their influence on the microstructure, and consequent the effects of twinning on mechanical properties of low Mg content Zn-Mg alloys.

## 2. Experimental

Pure Zn and Zn-Mg alloys were prepared by melting pure Zn (99.99%) and a Zn-30 wt%Mg alloy in a clay graphite crucible (dimension: 35 mm (bottom) x 65 mm (top) x 85 mm (height)) in a furnace at 500 °C, and the liquid metal was removed from the furnace and poured into moulds after 15 min of melting. Subsequently, the hot rolled Zn and Zn-(0.4, 0.8) wt% Mg (1 mm in thickness) were fabricated by multiple rolling passes at 250 °C.

Electrical discharge machining was used to prepare specimens for tensile testing (Dimensions: gauge length ~ 25 mm, width ~ 6 mm and thickness ~ 5 mm (as-cast Zn) and gauge length ~ 25 mm, width ~ 6 mm and thickness ~ 1 mm (hot-rolled Zn)) and while specimens for compression testing were machined from the as-cast materials with an ASTM standard (diameter of 13 mm and length of 38 mm) [32]. Also, to observe deformation induced microstructural changes during the tensile tests additional specimens with different dimensions were prepared from flat sheet material with a polished gauge length (Dimensions: gauge length ~ 25 mm, width ~ 6 mm and thickness ~ 2 mm). They were ground using SiC papers (P320-P4000), and the gauge length prepared by electro-polishing using a Struers® LectroPol-5 (Struers® D2 solution). The tensile tests were conducted in the longitudinal direction, i.e. parallel to the rolling direction, using an Instron single axis servo-hydraulic testing system. The crosshead speed was 1 mm/min for tensile testing and $10^{-3}s^{-1}$ for the compression tests. Microhardness was measured using a Struers® Duramin, with 0.05 Kg load.

A Struers® CitoPress-30 was employed to mount all metallographic samples, and grinding and polishing was conducted using a Struers® TegraPol-31. The samples were ground using SiC papers (P320-P4000) and they were polished to 1 μm. Finally, the samples were etched with Gennone-Kersey solution (1%HF, 15%$H_2SO_4$ and 84% distilled water) to observe the grain boundaries and deformation twinning. The microstructures were observed by POLYVAR optical microscope (OM) equipped with Spot 32 image analysis software. The linear intercept technique was used to calculate the average grain size of as-received materials [33]. A desktop SEM (Hitachi TM3030) was used to acquire Fracture morphology.

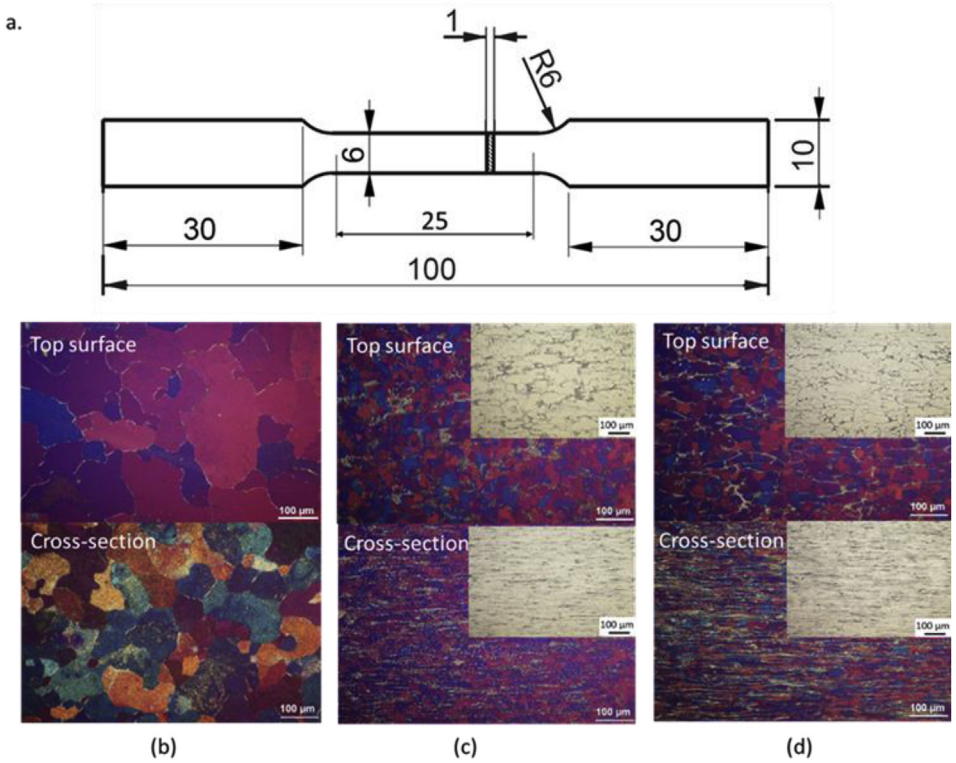


**Fig. 4.** The microstructure of as-rolled pure Zn and Zn-Mg alloys: (a) schematic of hot-rolled tensile specimens (GL: gauge length; W: width; T: thickness) (b) pure Zn, (c) Zn-0.4 wt%Mg and (d) Zn-0.8 wt%Mg. (The polarized micrographs are used to highlight grain structure and insets are used to show the eutectic phase).

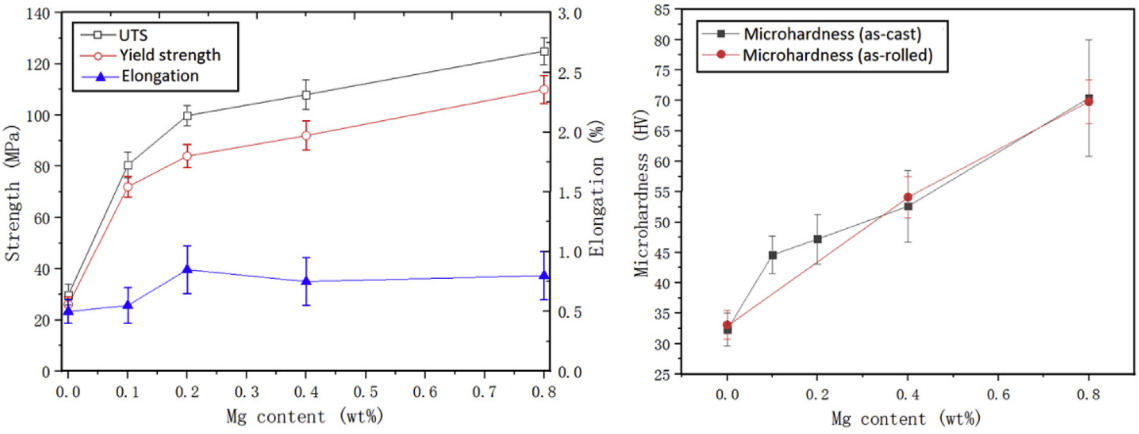


**Fig. 5.** (a) The tensile properties of as-cast pure Zn and Zn-Mg alloys (b) the microhardness of as-cast and as-rolled pure Zn and Zn-Mg alloys.

## 3. Results

### 3.1. Microstructure

Optical micrographs of as-cast samples are shown in Fig. 3. The pure Zn had a very coarse-grained structure (3094 ± 84 μm) which is refined appreciably as a result of alloying with 0.1 wt% Mg (160 ± 22 μm). Consequently, further grain refinement with the addition of increased levels of Mg is comparatively minor. As shown in Fig. 3, the grain size of the Zn-0.1 wt% is 160 ± 22 μm, which falls to 100 ± 25 μm, then 70 ± 11 μm and 65 ± 9 μm as the Mg content is increased to 0.2 wt%, 0.4 wt% and 0.8 wt%, respectively. An inter-dendritic eutectic phase is formed in the Zn-Mg alloys as shown on Fig. 3b–e (see insets top right). There is only limited proportions of the eutectic phase in the microstructure of the Zn-0.1 wt%Mg as the maximum solubility of Mg in Zn is around 0.1 wt%. Moreover, more substantial Mg contents lead to the formation of larger volume fractions of the eutectic phase and the dendritic structure of the η-Zn phase is readily apparent in the Zn-0.8 wt% Mg alloy as shown in Fig. 3e.

The microstructure of the hot-rolled Zn-Mg alloys is shown in Fig. 4. The grain structures were significantly refined by the hot rolling as compared to their as-cast counterparts. The average grain size of the as-rolled pure Zn is 121.6 μm (top-section) and 89.1 μm (cross-section), respectively (Fig. 4b). Also, the reduction in grain size of Zn-Mg alloys are significant up to 0.4 wt% Mg, but the further grain refinement with additions of Mg from 0.4 wt% to 0.8 wt% is negligible. The eutectic phase is shown in the inset images (Fig. 4c and d) but unlike the cast alloys the eutectic phase no longer constitutes a continuous network along the grain boundaries. The original network of eutectic phase (Fig. 3b–e) is broken down as a result of the hot rolling and dynamic recrystallization (DRX) at elevated temperature into fragmented particles which are elongated parallel to the rolling direction after several

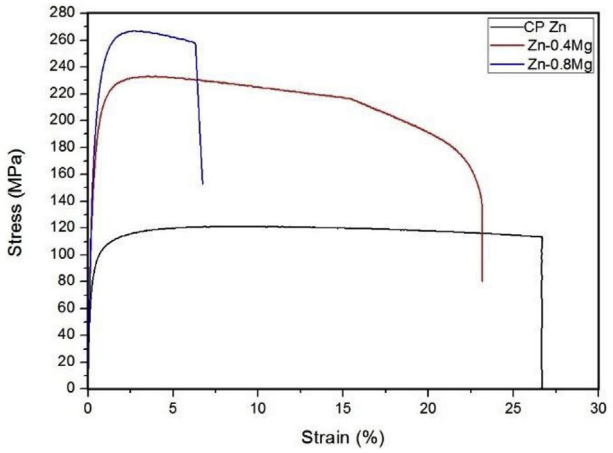


**Fig. 6.** Tensile stress-strain curves for hot rolled pure Zn and Zn-Mg alloys.

rolling passes.

### 3.2. Mechanical properties

The mechanical properties of the as-cast pure Zn and Zn-Mg alloys are shown in Fig. 5. The mechanical properties of as-cast pure Zn are relatively low (UTS ~ 29.7 MPa, yield strength (YS) ~ 27.5, $\varepsilon$ ~ 0.62% and microhardness ~ 32.7 HV), while the strength and microhardness increased markedly when alloyed with 0.1 wt% Mg (UTS ~ 81.5 MPa, YS ~ 72 MPa and, microhardness ~ 45.2 HV). With greater additions of Mg, the strength of the Zn-Mg alloys show further improvements with values of UTS ~ 120 MPa, YS ~ 112 MPa and microhardness ~ 71.1 HV for the Zn-0.8 wt%Mg alloy. Meanwhile, the ductility is relatively poor and shows only negligible variation with increased Mg contents.

The impacts of hot rolling on the properties of the pure Zn and Zn-Mg alloys are revealed in Fig. 6. The strength and ductility of pure Zn (UTS ~ 118 MPa, YS ~ 85 MPa and $\varepsilon$ ~ 26.8%) are improved considerably after hot rolling. Of particular note the ductility is increased almost 50 fold in comparison to the as-cast material. With additions of Mg, the strength is further increased for the Zn-0.4 wt%Mg (UTS ~ 230 MPa and YS ~ 225 MPa) and Zn-0.8 wt%Mg (UTS ~ 268 MPa and YS ~ 260 MPa) alloys, while the microhardness of the as-rolled specimens is similar to the as-cast specimens which indicates that the reduction of grain size has minor/no effects on microhardness (Fig. 5b). The hot rolled Zn-Mg alloys also show a significant improvement in ductility over their as-cast counterparts with an elongation up to necking of 16% and a total elongation around 23% for the Zn-0.4 wt%Mg alloy and total elongation of 7.2% for the 0.8 wt %Mg alloy.

### 3.3. Fractography

Fig. 7 shows the fracture surfaces of the as-rolled pure Zn and Zn-Mg alloys as well as for the cast counterpart to the Zn-0.4 wt%Mg alloy. The cast Zn-0.4 wt%Mg alloy displays features typical of a completely brittle fracture including a completely transgranular fracture interface with faceted, smooth surface textures and little evidence of plastic deformation associated with the failure (Fig. 7a), consistent with its poor elongation performance. The fracture surface of the as-rolled pure Zn show features typical of ductile fracture including dimpling across the entire fracture interface in keeping with its excellent elongation performance (Fig. 7b). In the case of the as-rolled Zn-0.4 wt%Mg alloy shown in Fig. 7c, cleavage planes are visible with fewer dimples in comparison to the pure Zn, indicative of a quasi-cleavage fracture surface representative of a mixed brittle and ductile failure with considerable elongation in the tensile testing. For the Zn-0.8 wt%Mg alloy, the fracture surface reveals brittle fracture features with cleavage planes dominating the fracture interface and negligible dimpling.

## 4. Discussion

Grain refinement observed in the cast samples with the addition of Mg is attributed to the growth restriction imparted by the Mg solute and to the promotion of heterogeneous nucleation on intermetallic particles formed in the melt during cooling [34]. The maximum solubility of Mg in Zn is 0.1 wt%, which is consistent with the microstructure of the Zn-0.1 wt%Mg alloy shown in Fig. 3b in that there are no substantive regions of the eutectic phase. As previously mentioned $Mg_2Zn_{11}$ is the only intermetallic compound in the Zn-Mg (Mg ≤ 3 wt%) alloys, and the eutectic point (6.3 wt%) for the $MgZn_2$ eutectic phase is in excess of 3 wt% Mg (Fig. 1). It has been reported that $MgZn_2$ particles form during casting in the initial stages of solidification, before the η-Zn phase forms at 466.1 °C. This is because the Zn-30 wt%Mg master alloy dissolves in the Zn melt gradually, and thus the local composition can be significantly higher than the nominal Mg content in the alloy which enables the $MgZn_2$ phase to form [34]. Consequently, the $MgZn_2$ particles provide efficient heterogeneous nucleation sites to refine the grain structure of the Zn-0.1%Mg alloy. Therefore, the significant improvement in mechanical properties of the Zn-0.1 wt%Mg alloy can be attributed to the solid solution strengthening imparted by the Mg and grain boundary (Hall–Petch) strengthening. Because the maximum solubility of Mg in Zn is 0.1 wt%, further addition of Mg has no significant influence on grain refinement. However, with the addition of further Mg the volume fraction of eutectic phase is increased which in turn leads to further reductions in the grain size [15]. As Fig. 3 shows, additions of Mg above 0.1 wt% promote formation of the eutectic phase along grain boundaries. Previous studies suggest that the eutectic phase can contribute to grain refinement by blocking the growth of Zn crystals [17]. Additionally, the microhardness of Zn-Mg alloys increases with increasing additions of Mg as the $Mg_2Zn_{11}$ is 4.7 times harder than pure Zn [35]. Meanwhile, the error range for the microhardness measurements on the as-cast specimens increased with the addition of Mg due to the inhomogeneous distribution of the eutectic phase. In contrast, the error range for the microhardness of the as-rolled specimens is much smaller because the eutectic phase is distributed more uniformly throughout the microstructure by the rolling process. Moreover, the microhardness of the as-rolled specimens is similar to the cast counterparts, which indicates that the significant reduction of grain size has minor effects on microhardness.

There was no significant changes in ductility with the addition of Mg to the as-cast alloys. The brittle and hard intermetallic constituent of the eutectic phase is reported to negatively impact on the ductility of the Zn-Mg alloys [15]. However, despite the significant refinement of the microstructure and only limited amounts of eutectic phase present in the Zn-0.1 wt%Mg alloy, the ductility remains low. Also, the propensity for twinning of the Zn-Mg alloys is substantially reduced in comparison to Zn due to restrictions on their formation resulting from the much smaller grain size (Fig. 3b) [31]. Both of these factors have been reported to have positive effects on the ductility of Zn based alloys [26,31], though this is not consistent with the poor elongation obtained for the Zn-0.1 wt%Mg in the tensile tests. Fig. 8 shows micrographs of the as-cast Zn-Mg alloys after the tensile tests. Compared with Fig. 3, there is profuse twinning evident which is concentrated around the fracture interface and even dominates the microstructure in the Zn-0.1 wt%Mg and Zn-0.2 wt%Mg alloys. The high propensity for twinning is attributed to cooperative contributions related to Poisson's effect and the twinning mode which is active in Zn-Mg alloys [26,36]. Poisson's effect dictates that tension along the longitudinal direction will impart compressive forces in the transverse direction [36]. Therefore, the compression accompanying the longitudinal extension promotes contraction twinning around the fracture interface. This is supported by the results shown in Fig. 9 which displays profuse twinning in the as-cast Zn-Mg alloys after compression testing. The twins are deduced to be

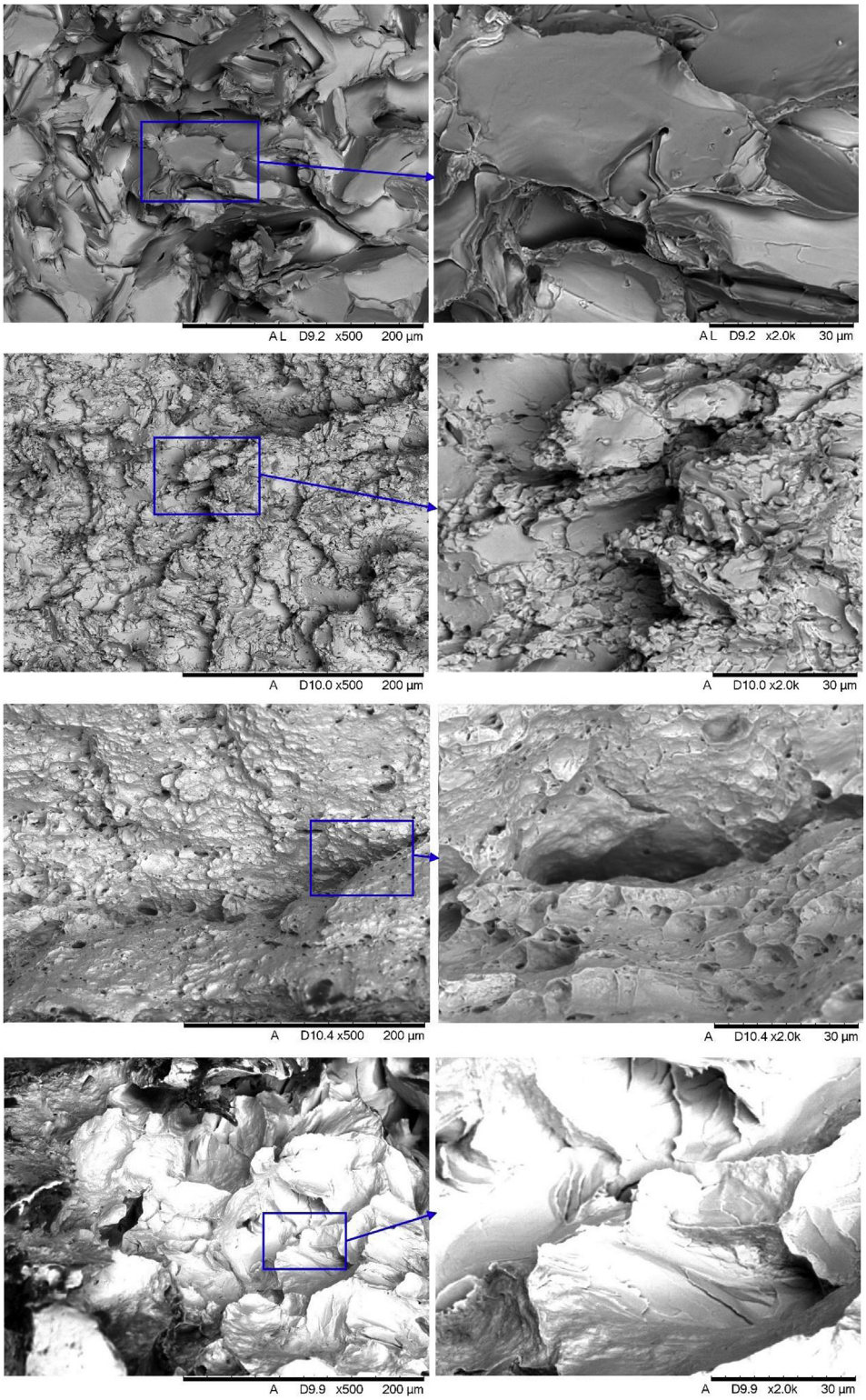


**Fig. 7.** SEM fracture surface for tensile specimens of (a) the as-cast Zn-0.4 Mg alloy, the (b) as-rolled pure Zn, (c) as-rolled Zn-0.4 Mg alloy, and (d) as-rolled Zn-0.8 Mg alloy.

$\{10\bar{1}2\} < 10\bar{1}\bar{1} >$ type twins. Yoo [26] has shown that for HCP metals with poor ductility, such as in the present study (Fig. 5a), only have the most general twinning mode, $\{10\bar{1}2\} < 10\bar{1}\bar{1} >$ type twinning, is active. In addition, the deformation twinning is concentrated near the fracture because the brittle eutectic network is resistant to plastic deformation and obstructs twinning. This is particularly evident for the Zn-0.4 wt% Mg.

Fig. 10 shows the microstructures after deformation of the as-cast Zn-0.2 wt%Mg alloy. The gauge length of the specimens was electro-polished prior to conducting the tensile tests. The elongation of these specimens was higher than the unpolished tensile specimens due to removal of surface defects through the polishing. A few small twins can be observed before the tensile tests which are attributed to surface deformations which occurred during manual grinding and polishing

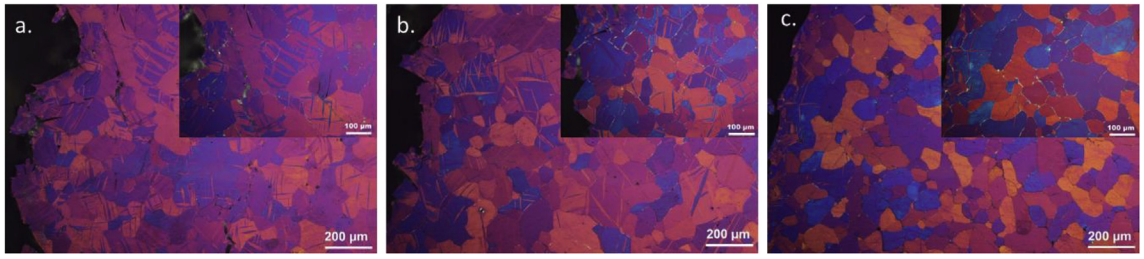


**Fig. 8.** Microstructures of the specimens near the fracture (in the mid-section of specimens) of as-cast Zn-Mg alloys after the tensile tests: (a) Zn-0.1 wt%Mg, (b) Zn-0.2 wt%Mg and (c) Zn-0.4 wt%Mg. (Insets are used to highlight fracture interface).

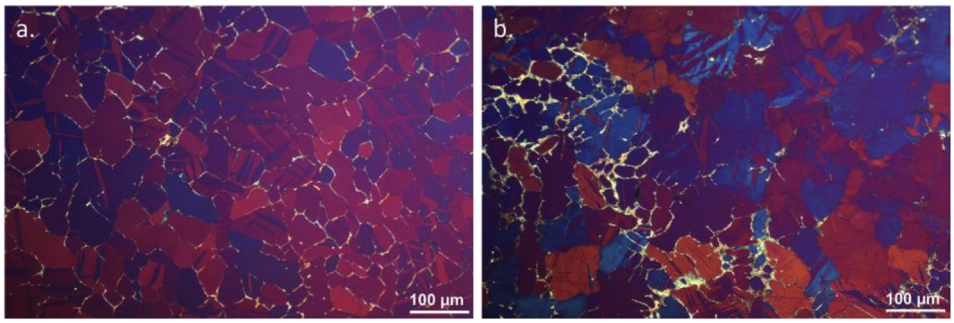


**Fig. 9.** The microstructure of cross-section of as-cast Zn-Mg alloys reduced 15% in the compression testing (a) Zn-0.4 wt%Mg and (b) Zn-0.8 wt%Mg.

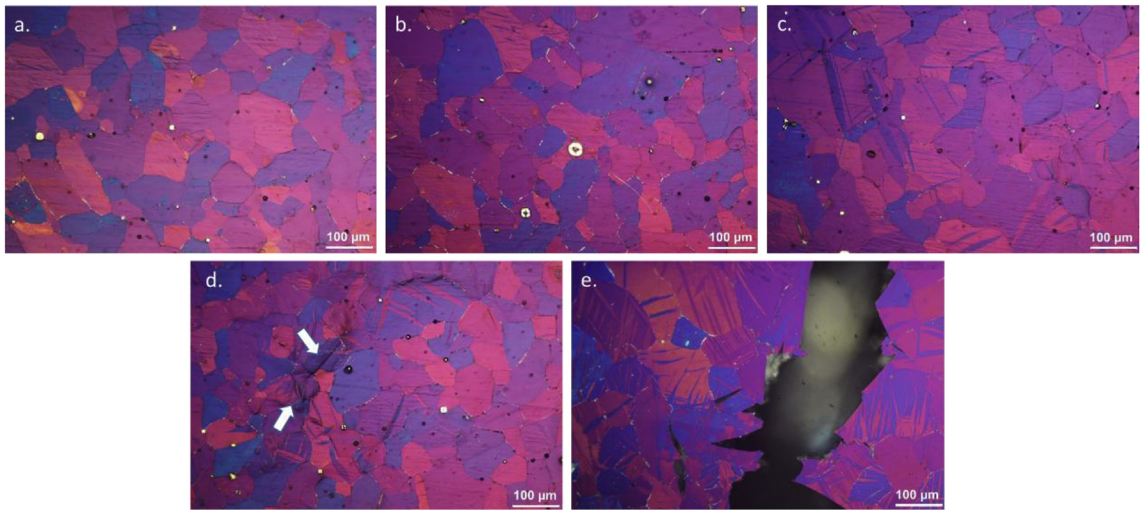


**Fig. 10.** The microstructural development during tensile deformation of Zn-0.2 wt%Mg (prepared by electro polishing before the the tensile tests): (a) before the testing, (b) strain to 0.8%, (c) strain to 1.0%, (d) strain to 1.2% and (e) strain to break (1.6%).

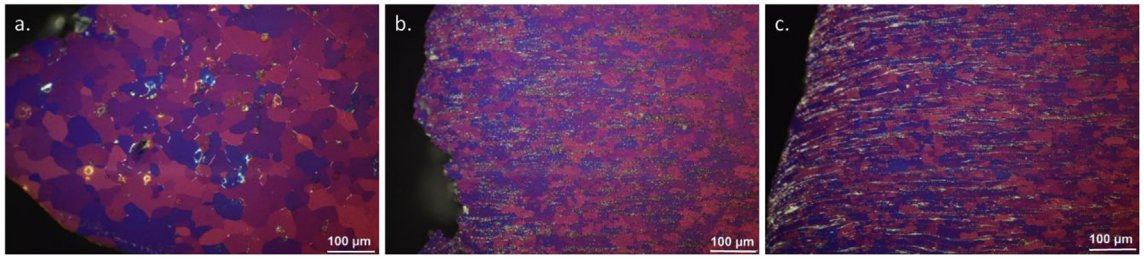


**Fig. 11.** Microstructures of the cross-section of as-rolled Zn-Mg alloys after the tensile tests, (a) pure zinc, (b) Zn-0.4 wt%Mg and (c) Zn-0.8 wt%Mg.

(Fig. 10a). There are no significant differences in the microstructure after straining to 0.8% (Fig. 10b) to that of the unstrained specimen. With further strain up to 1% (Fig. 10c), the proportion of twinning increased dramatically in the mid-section of the gauge length of the specimen and numerous examples of the impingement of twins is observed. Further straining up to 1.2%, resulted in the appearance of cleavage cracks at the location of the impinged twins (Fig. 10d). Finally, the specimen broke (strain to 1.6%) and profuse twinning is observed concentrated around the fracture. Fig. 8 shows that there is no longitudinal cracks, which if present are generally attributed to the reaction

of basal slip and pyramidal slip [37]. Moreover, the impingements of twinning in the brittle materials with only one active twinning mode causes local stress concentration that facilitated the crack nucleation and growth in the transverse direction [26]. Local stress concentrations promote the nucleation of twins and further accelerate the crack propagation [38]. Hence, deformation twinning is considered an important factor which limits ductility in Zn-Mg alloys.

The significant improvement in the strength of the as-rolled specimens is primarily due to effective grain refinement and the elimination of the casting defects [23]. The large primary Zn grains of the cast alloys are replaced by the uniform small equiaxed grains after rolling and the crystallographic orientation is rearranged along the rolling direction (Fig. 11). Additionally, the comprehensive grain refinement is attributed to the effects of dynamic recovery and dynamic recrystallisation (DRX) [17]. In the Zn-0.4 wt%Mg alloy, the eutectic phase obstructs the grain movement and grain growth, and the $Mg_2Zn_{11}$ intermetallic particles stimulate grain nucleation in the high-stress zone, which further accelerate DRX and results in more effective grain refinement [17,39]. There is no noticeable grain refinement with increases in the Mg content to 0.8 wt% (Fig. 11b and c). This is consistent with findings from Mostaed et al. [15] whom found that the effect of the addition of Mg above 0.5 wt% on the grain size of extruded Zn-Mg alloys was minor. As was discussed in section 3.1, after rolling a continuous eutectic network is no longer present along the grain boundaries. The continuous eutectic network in the as-cast Zn-Mg alloys is broken down into smaller aggregates in the rolling and is aligned to the rolling direction. The refined eutectic acts as a substantive barrier to further twinning. Meanwhile, grain boundary strengthening is increased substantially by the hot rolling. The grain boundaries also restrict further twinning, which otherwise causes high localised stress concentrations around impinging twins and accelerates crack nucleation (Fig. 11), resulting in improved plastic deformation and elongation such as observed for the Zn-0.4 wt%Mg alloy [39]. The significantly lower ductility of the hot rolled Zn-0.8 wt%Mg is attributed to the presence of the network of brittle and hard eutectic intermetallic phase around the deformed and DRX Zn grains facilitating the initiation and growth of cracks before significant plastic deformation can occur [17].

## 5. Conclusion

Investigations on the role of twinning in tensile deformation of Zn-Mg alloys and consequent effects of twinning on mechanical properties in the present study reveal the following findings:

1. In the as-cast Zn-Mg alloys, the propensity for twinning is reduced significantly with increasing levels of Mg addition ($\leq$0.8 wt%), because of the smaller grain size and significant volume fraction of eutectic phase which inhibits twinning.
2. Deformation twinning has adverse effects on the ductility of as-cast Zn-Mg alloys. There is no twinning in the initial stages of tensile deformation, and the propensity for twinning increases suddenly at around 1% strain and twinning impingements are observed. With further strain, the propensity for twinning and impingements increases and profuse twinning and impingements are observed on fracture (strain to 1.6%). The associated compressive strain in tension facilitates $\{10\bar{1}2\} < 10\bar{1}\bar{1} >$ contraction twinning leading to twinning impingements, which in turn cause local stress concentrations which faciliate crack nucleation and growth.
3. As-rolled Zn-Mg alloys have much better strength and ductility which is attributed to grain refinement, elimination of casting defects and grain boundary sliding, respectively. Additionally, the presence of a eutectic intermetallic network, strong grain boundaries and small grain size inhibit twinning in tensile deformation which otherwise would initiate cracking. With the addition of Mg contents > 0.4 wt%, the brittle and hard $Mg_2Zn_{11}$ intermetallic phase has adverse impacts on ductility.

## Acknowledgment

Authors are grateful to Mr. Nagasivamuni Balasubramani and Ms. Lihui Zheng for their assistance for materials and metallographic samples preparation. Centre for Advanced Materials Processing and Manufacturing (AMPAM) and the ARC Research Hub for Advanced Manufacturing of Medical Devices are gratefully acknowledged for financial support.

## References

[1] M. Saini, Y. Singh, P. Arora, V. Arora, K. Jain, Implant biomaterials: a comprehensive review, World J. Clin. Cases 3 (1) (2015) 52–57 https://doi.org/10.12998/wjcc.v3.i1.52.
[2] A. Illarionov, S. Belikov, S. Grib, A. Yurovskikh, Metallic materials for medical use, MATEC Web of Conferences. XIII International Scientific-technical Conference “Dynamic of Technical Systems” (DTS-2017), vol. 132, 2017 03003 https://doi.org/10.1051/matecconf/201713203003.
[3] J.-M. Seitz, M. Durisin, J. Goldman, J.W. Drelich, Recent advances in biodegradable metals for medical sutures: a critical review, Adv. Healthc. Mater. 4 (2015) 1915–1936 https://doi.org/10.1002/adhm.201500189.
[4] G.K. Levy, J. Goldman, E. Aghion, The prospects of zinc as a structural material for biodegradable implants-A review paper, Metals 7 (10) (2017) 402 https://doi.org/10.3390/met7100402.
[5] H. Yang, C. Wang, C. Liu, H. Chen, Y. Wu, J. Han, Z. Jia, W. Lin, D. Zhang, W. Li, W. Yuan, H. Guo, H. Li, G. Yang, D. Kong, D. Zhu, K. Takashima, L. Ruan, J. Nie, X. Li, Y. Zheng, Evolution of the degradation mechanism of pure zinc stent in the one-year study of rabbit abdominal aorta model, Biomaterials 145 (2017) 92–105 https://doi.org/10.1016/j.biomaterials.2017.08.022.
[6] Y. Chen, Z. Xu, C. Smith, J. Sankar, Recent advances on the development of magnesium alloys for biodegradable implants, Acta Biomater. 10 (2014) 4561–4573 https://doi.org/10.1016/j.actbio.2014.07.005.
[7] K. Hanada, K. Matsuzaki, X. Huang, Y. Chino, Fabrication of Mg alloy tubes for biodegradable stent application, Mater. Sci. Eng. C 33 (2013) 4746–4750 https://doi.org/10.1016/j.msec.2013.07.033.
[8] S. Agarwal, J. Curtin, B. Duffy, S. Jaiswal, Biodegradable magnesium alloys for orthopaedic applications: a review on corrosion, biocompatibility and surface modifications, Mater. Sci. Eng. C 68 (2016) 948–963 https://doi.org/10.1016/j.msec.2016.06.020.
[9] Y.B. Wang, H.F. Li, Y.F. Zheng, M. Li, Corrosion performances in simulated body fluids and cytotoxicity evaluation of Fe-based bulk metallic glasses, Mater. Sci. Eng. C 32 (2011) 599–606 https://doi.org/10.1016/j.msec.2011.12.018.
[10] J. Cheng, B. Liu, Y.H. Wu, Y.F. Zheng, Comparative invitro study on pure metals (Fe, Mn, Mg, Zn and W) as biodegradable metals, J. Mater. Sci. Technol. 29 (2013) 619–627.
[11] Y.F. Zheng, X.N. Gu, F. Witte, Biodegradable metals, Mater. Sci. Eng. R Rep. 77 (2014) 1–34 https://doi.org/10.1016/j.mser.2014.01.001.
[12] H. Gong, K. Wang, R. Strich, J.G. Zhou, In vitro biodegradation behavior, mechanical properties, and cytotoxicity of biodegradable Zn–Mg alloy, J. Biomed. Mater. Res. B Appl. Biomater. 103 (2015) 1632–1640 https://doi.org/10.1002/jbm.b.33341.
[13] D. Zhu, Y. Su, M.L. Young, J. Ma, Y. Zheng, L. Tang, Biological responses and mechanisms of human bone marrow mesenchymal stem cells to Zn and Mg biomaterials, ACS Appl. Mater. Interfaces 9 (2017) 27453–27461 https://doi.org/10.1021/acsami.7b06654.
[14] X. Gu, Y. Zheng, Y. Cheng, S. Zhong, T. Xi, In vitro corrosion and biocompatibility of binary magnesium alloys, Biomaterials 30 (2009) 484–498 https://doi.org/10.1016/j.biomaterials.2008.10.021.
[15] E. Mostaed, M. Sikora-Jasinska, A. Mostaed, S. Loffredo, A.G. Demir, B. Previtali, D. Mantovani, R. Beanland, M. Vedani, Novel Zn-based alloys for biodegradable stent applications: design, development and in vitro degradation, J. Mech. Behav. Biomed. Mater. 60 (2016) 581–602 https://doi.org/10.1016/j.jmbbm.2016.03.018.
[16] X. Liu, J. Sun, Y. Yang, Z. Pu, Y. Zheng, In vitro investigation of ultra-pure Zn and its mini-tube as potential bioabsorbable stent material, Mater. Lett. 161 (2015) 53–56 https://doi.org/10.1016/j.matlet.2015.06.107.
[17] J. Kubásek, D. Vojtěch, E. Jablonská, I. Pospíšilová, J. Lipov, T. Ruml, Structure, mechanical characteristics and in vitro degradation, cytotoxicity, genotoxicity and mutagenicity of novel biodegradable Zn–Mg alloys, Mater. Sci. Eng. C 58 (2016) 24–35 https://doi.org/10.1016/j.msec.2015.08.015.
[18] X. Liu, J. Sun, Y. Yang, F. Zhou, Z. Pu, L. Li, Y. Zheng, Microstructure, mechanical properties, in vitro degradation behavior and hemocompatibility of novel Zn–Mg–Sr alloys as biodegradable metals, Mater. Lett. 162 (2016) 242–245 https://doi.org/10.1016/j.matlet.2015.07.151.
[19] S. Zhao, J.-M. Seitz, R. Eifler, H.J. Maier, R.J. Guillory II, E.J. Earley, A. Drelich, J. Goldman, J.W. Drelich, Zn-Li alloy after extrusion and drawing: structural, mechanical characterization, and biodegradation in abdominal aorta of rat, Mater. Sci. Eng. C 76 (2017) 301–312 https://doi.org/10.1016/j.msec.2017.02.167.
[20] C. Yao, Z. Wang, S.L. Tay, T. Zhu, W. Gao, Effects of Mg on microstructure and corrosion properties of Zn–Mg alloy, J. Alloy. Comp. 602 (2014) 101–107 https://doi.org/10.1016/j.jallcom.2014.03.025.
[21] M. Dutta, A.K. Halder, S.B. Singh, Morphology and properties of hot dip Zn–Mg and

Zn–Mg–Al alloy coatings on steel sheet, Surf. Coating. Technol. 205 (2010) 2578–2584 https://doi.org/10.1016/j.surfcoat.2010.10.006.
[22] J. Kubásek, I. Pospíšilová, D. Vojtěch, E. Jablonská, T. Ruml, Structural, mechanical and cytotoxicity characterization of as-cast biodegradable Zn-xMg (x = 0.8-8.3 %) alloys, Mater. Technol. 48 (2014) 623–629.
[23] D. Vojtěch, J. Kubásek, J. Šerák, P. Novák, Mechanical and corrosion properties of newly developed biodegradable Zn-based alloys for bone fixation, Acta Biomater. 7 (2011) 3515–3522 https://doi.org/10.1016/j.actbio.2011.05.008.
[24] X. Liu, J. Sun, F. Zhou, Y. Yang, R. Chang, K. Qiu, Z. Pu, L. Li, Y. Zheng, Micro-alloying with Mn in Zn–Mg alloy for future biodegradable metals application, Mater. Des. 94 (2016) 95–104 https://doi.org/10.1016/j.matdes.2015.12.128.
[25] A. Dong, B. Li, Y. Lu, G. Zhu, H. Xing, D. Shu, B. Sun, J. Wang, Effect of Mg on the microstructure and corrosion resistance of the continuously hot-dip galvanizing Zn-Mg coating, Materials 10 (2017) 980 https://doi.org/10.3390/ma10080980.
[26] M.H. Yoo, Slip, twinning, and fracture in hexagonal close-packed metals, Metall. Trans. A 12 (1981) 409–418 https://doi.org/10.1007/BF02648537.
[27] X. Liao, J. Wang, J. Nie, Y. Jiang, P. Wu, Deformation twinning in hexagonal materials, MRS Bull. 41 (2016) 314–319 https://doi.org/10.1557/mrs.2016.64.
[28] T.B. Britton, F.P.E. Dunne, A.J. Wilkinson, On the mechanistic basis of deformation at the microscale in hexagonal close packed metals, Proc. R. Soc. A (2015) 471 https://doi.org/10.1098/rspa.2014.0881.
[29] G. Dirras, J. Gubicza, H. Couque, A. Ouarem, P. Jenei, Mechanical behaviour and underlying deformation mechanisms in coarse- and ultrafine-grained Zn over a wide range of strain rates, Mater. Sci. Eng., A 564 (2013) 273–283 https://doi.org/10.1016/j.msea.2012.12.010.
[30] J. Tu, S. Zhang, On the $\{10\bar{1}2\}$ twinning growth mechanism in hexagonal close-packed metals, Mater. Des. 96 (2016) 143–149 https://doi.org/10.1016/j.matdes.2016.02.002.
[31] N. Ecob, R. Brian, The effect of grain size on deformation twinning in a textured zinc alloy, J. Mater. Sci. 18 (1983) 2419–2429 https://doi.org/10.1007/BF00541848.
[32] ASTM E9-09 Standard Test Methods of Compression Testing of Metallic Materials at Room Temperature, ASTM International, West Conshohocken, PA, 2009https://doi.org/10.1520/E0009-09 https://compass.astm.org.
[33] ASTM E112-10 Standard Test Methods for Determining Average Grain Size, ASTM International, West Conshohocken, PA, 2010https://doi.org/10.1520/E0112-10 https://compass.astm.org.
[34] Z. Liu, D. Qiu, F. Wang, J.A. Taylor, M. Zhang, Grain refinement of cast zinc through magnesium inoculation: characterisation and mechanism, Mater. Char. 106 (2015) 1–10 https://doi.org/10.1016/j.matchar.2015.05.011.
[35] C.C. Kammerer, S. Behdad, L. Zhou, F. Betancor, M. Gonzalez, B. Boesl, Y.H. Sohn, Diffusion kinetics, mechanical properties, and crystallographic characterization of intermetallic compounds in the Mg–Zn binary system, Intermetallics 67 (2015) 145–155 https://doi.org/10.1016/j.intermet.2015.08.001.
[36] G.N. Greaves, A.L. Greer, R.S. Lakes, T. Rouxel, Poisson's ratio and modern materials, Nat. Mater. 10 (2011) 823–837 https://doi.org/10.1038/nmat3134.
[37] B.J. Burr, N. Thompson, Dislocations and cracks in zink, Philos. Mag. A 7 (1962) 1773–1778 https://doi.org/10.1080/14786436208213709.
[38] S. Sinha, N.P. Gurao, In situ electron backscatter diffraction study of twinning in commercially pure titanium during tension-compression deformation and annealing, Mater. Des. 116 (2017) 686–693 https://doi.org/10.1016/j.matdes.2016.10.060.
[39] A. Jarzębska, M. Bieda, J. Kawałko, L. Rogal, P. Koprowski, K. Sztwiertnia, W. Pachla, M. Kulczyk, A new approach to plastic deformation of biodegradable zinc alloy with magnesium and its effect on microstructure and mechanical properties, Mater. Lett. 211 (2018) 58–61 https://doi.org/10.1016/j.matlet.2017.09.090.